

# Unusual Dynamics and $pK_a$ Shift at the Active Site of a Lead-Dependent Ribozyme<sup>‡</sup>

Pascale Legault<sup>†</sup> and Arthur Pardi\*

Contribution from the Department of Chemistry and Biochemistry, University of Colorado at Boulder, Boulder, Colorado 80309-0215

Received November 18, 1996. Revised Manuscript Received April 25, 1997<sup>⊗</sup>

**Abstract:** Heteronuclear NMR spectroscopy has been used to probe the structure and dynamics of a lead-dependent ribozyme known as the leadzyme. The  $pK_a$ 's for all adenine bases in the leadzyme were measured and vary from <3.1 to 6.5. The adenines with the lowest  $pK_a$ 's are involved in Watson–Crick base pairs, and the adenine with the highest  $pK_a$  is thought to form an  $AH^+–C$  wobble base pair at the active site of the leadzyme. The potential structural and functional significance associated with perturbed  $pK_a$ 's in ribozymes is discussed. NMR studies of 5' AMP, 5' CMP, 5' GMP, and 5' UMP were also used to identify the <sup>13</sup>C resonances that represent the best probes of base protonation for all four bases in RNA. The line width of the C2 resonance of the adenine with a  $pK_a$  of 6.5 was analyzed to probe the dynamics of the catalytically active internal loop in the leadzyme. These results showed that this adenine is undergoing a chemical exchange process with a lifetime of  $\sim 30 \mu s$  and demonstrate rapid dynamics at the active site of this ribozyme. Thus <sup>13</sup>C NMR can be used to probe dynamic processes in RNA oligomers.

## Introduction

Proton transfer plays a critical role in many protein enzymatic reactions and the ability to determine the  $pK_a$  of an ionizable side-chain group has been important for understanding the molecular mechanism of many protein enzymes.<sup>1</sup> In contrast to proteins, nucleic acids are anionic polymers made up of monomers that do not contain functional groups with  $pK_a$ 's near physiological pH. Therefore one might conclude that nucleic acids are unlikely to undergo pH-induced transitions near physiological pH. However, structural studies on various nucleic acids have revealed adenine and cytidine  $pK_a$ 's that differ significantly from the  $pK_a$ 's of the monomers.<sup>2–14</sup> In addition, many modified nucleosides in naturally occurring RNAs possess a net positive charge at neutral pH.<sup>15,16</sup> For example, in yeast

tRNA<sup>Phe</sup> the protonated m<sup>7</sup>G<sub>46</sub> is part of a triple base interaction, and the protonated m<sup>1</sup>A<sub>58</sub> forms a reversed Hoogsteen base pair with T<sub>54</sub>.<sup>15</sup> These two non-Watson–Crick base interactions involve invariant or semiinvariant bases that stabilize the tertiary structure of tRNAs.<sup>15</sup> These findings indicate that ionizable groups are likely to be important for the function and structure of nucleic acids.

The ability to prepare milligram quantities of uniformly <sup>13</sup>C/<sup>15</sup>N-labeled RNA oligomers of defined sequence has allowed many heteronuclear magnetic resonance techniques, initially developed for proteins, to be applied to nucleic acids and has also prompted the development of new NMR experiments specifically designed for assignment and structure determination of RNA (see ref 17 for a review). In addition to simplifying the structure determination of RNA, NMR studies of isotopically labeled RNA can also yield information on the function and dynamics of RNA. For example, we recently described a <sup>13</sup>C NMR method for measuring adenine  $pK_a$ 's in nucleic acids.<sup>5</sup> This technique was used to identify an unusual  $pK_a$  of 6.5 for an adenine at the active site of a lead-dependent ribozyme known as the leadzyme.<sup>18,19</sup> The work presented here extends that study by describing <sup>13</sup>C NMR probes that can be used to determine the  $pK_a$ 's of all four natural bases in RNA. The effect of imino protonation on the base <sup>13</sup>C chemical shifts and <sup>1</sup>J<sub>CH</sub> coupling constants in 5' AMP, 5' CMP, 5' GMP, and 5' UMP have been determined. The  $pK_a$ 's for all adenines in the leadzyme have been measured, and <sup>13</sup>C NMR experiments also showed that there are no cytidine bases with unusually high  $pK_a$ 's. The potential structural and functional significance associated with perturbed  $pK_a$ 's in ribozymes is discussed.

Many NMR structure determinations of macromolecules show significant local dynamics and another important application of NMR spectroscopy is probing the dynamics of molecules in

\* Author to whom correspondence should be addressed.

<sup>†</sup> Present address: Department of Medical Genetics and Microbiology, One King's College Circle, University of Toronto, Toronto, Ontario, M5S 1A8, Canada.

<sup>‡</sup> Keywords: RNA structure,  $pK_a$ , chemical exchange, NMR, dynamics, ribozyme.

<sup>⊗</sup> Abstract published in *Advance ACS Abstracts*, July 1, 1997.

(1) Fersht, A. *Enzyme Structure and Mechanism*; W. H. Freeman: New York, 1984; pp 1–475.

(2) Macaya, R. F.; Gilbert, D. E.; Shiva, M.; Sinsheimer, J. S.; Feigon, J. *Science* **1991**, *254*, 270–274.

(3) Boulard, Y.; Cognet, J. A. H.; Gabarro-Arpa, J.; Le Bret, M.; Sowers, L. C.; Fazakerley, G. V. *Nucleic Acids Res.* **1992**, *20*, 1933–1941.

(4) Wang, C.; Gao, H.; Gaffney, B. L.; Jones, R. A. *J. Am. Chem. Soc.* **1991**, *113*, 5486–5488.

(5) Legault, P.; Pardi, A. *J. Am. Chem. Soc.* **1994**, *116*, 8390–8391.

(6) Puglisi, J. D.; Wyatt, J. R.; Tinoco, I., Jr. *Biochemistry* **1990**, *29*, 4215–4226.

(7) Dolinnaya, N. G.; Fresco, J. R. *Proc. Natl. Acad. Sci. U.S.A.* **1992**, *89*, 9242–9246.

(8) Gao, X.; Patel, D. J. *J. Am. Chem. Soc.* **1988**, *110*, 5178–5182.

(9) Liu, K.; Miles, H. T.; Frazier, J.; Sasisekharan, V. *Biochemistry* **1993**, *32*, 11802–11809.

(10) Leroy, J.-L.; Gehring, K.; Kettani, A.; Guéron, M. *Biochemistry* **1993**, *32*, 6019–6631.

(11) Jaishree, T. N.; Wang, A. H.-J. *Nucleic Acids Res.* **1993**, *21*, 3839–3844.

(12) Connell, G. J.; Yarus, M. *Science* **1994**, *264*, 1137–1141.

(13) Kao, T. H.; Crothers, D. M. *Proc. Natl. Acad. Sci. U.S.A.* **1980**, *77*, 3360–3364.

(14) Cai, Z.; Tinoco, I., Jr. *Biochemistry* **1996**, *35*, 6026–6036.

(15) Saenger, W. *Principles of Nucleic Acid Structure*; Springer-Verlag: New York, 1984; pp 556.

(16) Limbach, P. A.; Crain, P. F.; McCloskey, J. A. *Nucleic Acids Res.* **1994**, *22*, 2183–2196.

(17) Pardi, A. *Methods Enzymol.* **1995**, *261*, 350–380.

(18) Pan, T.; Uhlenbeck, O. C. *Nature* **1992**, *358*, 560–563.

(19) Pan, T.; Dichtl, B.; Uhlenbeck, O. C. *Biochemistry* **1994**, *33*, 9561–9565.

solution.  $^{13}\text{C}$  or  $^{15}\text{N}$  relaxation data can be used to probe very rapid molecular motions in macromolecules (lifetimes  $\leq$   $\sim$ nanoseconds),<sup>20</sup> but it is not always clear how well these fast motions can be correlated with biological function. Slower molecular motions are often manifested as line broadening of specific resonances, which yields information on processes in the microsecond–millisecond timescale;<sup>21</sup> and such processes are more likely to have functional significance than subnanosecond processes. Observation of  $^{13}\text{C}$  and  $^{15}\text{N}$  resonances in isotopically labeled RNA provides additional timescales that expand the possibilities for probing the dynamics of RNA in solution. The  $^{13}\text{C}$  line widths in the uniformly  $^{13}\text{C}$  labeled leadzyme were analyzed, and these data provide novel information on the dynamics of the catalytically active internal loop in this molecule.

## Materials and Methods

**Preparation of  $^{13}\text{C}/^{15}\text{N}$ -Labeled 5' NMPs and  $^{13}\text{C}/^{15}\text{N}$ -Labeled Leadzyme Samples.** The 99%  $^{13}\text{C}/^{15}\text{N}$ -labeled NMPs were obtained from *E. coli* cells grown on minimal media containing 99%  $^{13}\text{C}$ -glucose (Isotec) and 99%  $^{15}\text{N}$ - $(\text{NH}_4)_2\text{SO}_4$  (Isotec) as described previously.<sup>22,23</sup> The four isotopically labeled NMPs were separated by anion exchange chromatography<sup>24</sup> using Dowex-1 anion exchange resin with 2% cross-linkage and 100–200 mesh size (Sigma). Nucleotide purity was assessed to be greater than 95% by optical/UV spectroscopy,  $^1\text{H}$  and  $^{13}\text{C}$  NMR spectroscopy, and HPLC on an analytical anion exchange nucleotide separation column (Vydac 303NT405). The 2 mM NMR samples of the  $^{13}\text{C}/^{15}\text{N}$ -NMPs were prepared in  $\text{D}_2\text{O}$ , and their pH's were adjusted using a glass electrode. A 0.44 mM NMR sample of 99%  $^{13}\text{C}/^{15}\text{N}$ -labeled leadzyme was prepared from a 20 mL *in vitro* transcription reaction containing 40 mM Tris pH 8.0, 20 mM  $\text{MgCl}_2$ , 5 mM DTT, 1 mM spermidine, 8 mM (160  $\mu\text{mol}$ )  $^{13}\text{C}/^{15}\text{N}$ -labeled NTPs, 0.1% Triton X-100, 0.2  $\mu\text{M}$  template, and 0.46 mg T7 RNA polymerase using standard procedures.<sup>23,25</sup> The gel-purified  $^{13}\text{C}/^{15}\text{N}$ -labeled leadzyme was dialyzed using a Centricon-3 concentrator (Amicon, Inc.) to a final buffer composition of 10 mM sodium phosphate, 0.2 mM EDTA, 0.1 M NaCl, and pH 5.5. The sample volume was brought to 550  $\mu\text{L}$  and transferred to 99.996%  $\text{D}_2\text{O}$  by multiple cycles of lyophilization and resuspension. A second 1.2 mM 99%  $^{13}\text{C}/^{15}\text{N}$ -labeled leadzyme was also prepared by a similar procedure. This sample is being used in structural studies, and the pH was kept at 5.5.

**pH Titrations.** pH values were measured in  $\text{D}_2\text{O}$  with a glass electrode and adjusted with 0.1 N DCl and 0.1 N NaOD. For the titration of the  $^{13}\text{C}/^{15}\text{N}$ -labeled 5' NMPs, a 2 mM sample of each NMP was prepared at each pH. For the 0.44 mM  $^{13}\text{C}/^{15}\text{N}$ -labeled leadzyme sample, two separate pH titrations were performed, one for measuring the  $\text{pK}_a$ 's of the adenine bases and a second for probing the dynamics for adenine 25. For measuring the  $\text{pK}_a$ 's, spectra were recorded on the same sample where the initial pH was 5.8, then adjusted by steps of  $\sim$ 0.5 pH units up to pH 8.3, brought down to pH 4.4, and adjusted by steps of  $\sim$ 0.5 pH units up to pH 5.8. The NMR spectra collected at pH 5.8 before and after the pH titration were identical within experimental error. In the pH titration for probing the dynamics, NMR spectra were collected at pH's of 4.20, 5.50, 5.85, 6.55, 7.63, and 8.45. The extreme pH values (4.20 and 8.45) are averages of the pH measured in  $\text{D}_2\text{O}$  with the glass electrode before and after the NMR experiment and have an error of  $\pm$ 0.05 pH unit. For the intermediate pH's on the 0.44 mM sample of the leadzyme (5.85  $\pm$  0.07, 6.55  $\pm$  0.05, 7.6  $\pm$  0.2) and for the 1.2 mM sample at pH 5.5  $\pm$  0.1, the pH of the solution was calculated from the value of the A25 C2 chemical shift assuming

an error of  $\pm$ 0.2 ppm in the  $^{13}\text{C}$  chemical shift.<sup>5</sup> After the NMR titrations, the integrity of the RNA sample was demonstrated by electrophoresis where only a single band was observed on a 20% denaturing polyacrylamide gel.

**NMR Spectroscopy.** The  $^{13}\text{C}$  chemical shifts for the  $^{13}\text{C}/^{15}\text{N}$ -labeled 5' NMPs were measured from 1D  $^1\text{H}$ -decoupled  $^{13}\text{C}$  NMR spectra recorded at 25  $^\circ\text{C}$ . The  $^{13}\text{C}$  resonances in the 5' NMPs have been previously assigned<sup>26</sup> and the chemical shifts measured here have an error of  $\pm$ 0.03 ppm. One-bond  $^1\text{H}$ – $^{13}\text{C}$  J coupling constants were obtained from 1D  $^1\text{H}$  NMR spectra recorded at 25  $^\circ\text{C}$ . For the  $^{13}\text{C}/^{15}\text{N}$ -labeled leadzyme or when there was overlap in the spectra of the 5' NMPs, the  $^{13}\text{C}$  chemical shifts were measured from 2D ( $^{13}\text{C}$ ,  $^1\text{H}$ ) HMQC spectra.<sup>27</sup> These spectra were recorded at 25  $^\circ\text{C}$  with 128 scans, the  $^1\text{H}$  carrier at 4.80 ppm and 2048 complex points with a sweep width of 6000 Hz in  $t_2$ , and the  $^{13}\text{C}$  carrier at 145.54 ppm and 180 complex points with a sweep width of 3000 Hz in  $t_1$ . Quadrature detection in  $t_1$  employed the States-TPPI method,<sup>28</sup> and  $^{13}\text{C}$  WALTZ-decoupling was applied during  $t_2$ . The total time of each HMQC experiment was 8.5 h. For the studies of the dynamics of the leadzyme, the line widths were measured from 1D  $^{13}\text{C}$  vectors of 2D ( $^{13}\text{C}$ ,  $^1\text{H}$ ) HSQC spectra at 25  $^\circ\text{C}$  transformed without the use of any weighing function. These HSQC spectra were recorded as above except that 192 scans were collected for 1024 complex points with a sweep width of 4200 Hz in  $t_2$ , and 108 complex points with a sweep width of 2600 Hz in  $t_1$ . The total time of each of these HSQC experiments was 21 h. The  $^1\text{H}$  chemical shifts were referenced to the internal HOD at 4.80 ppm, and the  $^{13}\text{C}$  chemical shifts were referenced to an external standard of TSP at 0.00 ppm. A 2.5 h 2D ( $^{13}\text{C}$ ,  $^1\text{H}$ ) HSQC spectrum was also collected on the 1.2 mM  $^{13}\text{C}/^{15}\text{N}$ -labeled leadzyme sample at pH 5.5, 25  $^\circ\text{C}$  in  $\text{D}_2\text{O}$ . To assign the C4 resonances in the cytidine residues, a triple resonance 2D (HN)C(CC)H spectrum was collected on the 1.2 mM leadzyme sample at pH 5.5, 25  $^\circ\text{C}$  in 90%  $\text{H}_2\text{O}/10\%$   $\text{D}_2\text{O}$ . The spectrum was acquired and processed as previously described,<sup>29</sup> except that the pulse sequence was modified to frequency label the C4 resonances in the evolution period. The NMR data were collected on Varian VXR-500S or Unityplus 500 spectrometers and processed with the program FELIX (Biosym Inc.).

**Determination of Adenine  $\text{pK}_a$ 's in the Leadzyme.** The  $\text{pK}_a$  determination was based on a Hill plot analysis for one-site protonation<sup>30</sup> using the equation  $\text{pH} = \log((1-\alpha)/\alpha) + \text{pK}_a$ , where  $\alpha$  represents the fraction of the protonated species. The value of  $\alpha$  is calculated from the change in C2 chemical shift relative to the unprotonated state at a given pH,  $\Delta$ , divided by the total change in chemical shift between the unprotonated and the protonated state,  $\Delta_T$ . This Henderson–Hasselbalch-type equation can then be rewritten as  $\text{pH} = \log((\Delta_T - \Delta)/\Delta) + \text{pK}_a$ . For A25, a complete pH titration curve was obtained in the range of pH studied (pH 4.4–8.3), and the  $\text{pK}_a$  value was solved by linear regression analysis of the Hill plot as described.<sup>5</sup> The  $\text{pK}_a$ 's of all other adenines were calculated from this Henderson–Hasselbalch equation at pH = 4.4 where  $\Delta$  is the difference in C2 chemical shift between pH = 8.3 and 4.4 (with an error of  $\pm$ 0.6 ppm on the difference in chemical shifts and  $\pm$ 0.3 ppm if there is no observed change) and where  $\Delta_T$  is the total change in chemical shift for protonation of 5' AMP (8.0  $\pm$  0.6 ppm).

**Determination of the Lifetime of Exchange.** The lifetimes for exchange were determined from an expression derived from the Bloch equations which defines the NMR signal lineshape for a two-site (A and B) chemically-exchanging system. Equation 1 is an extension of previous work,<sup>31</sup> where here the line widths of the two states were not assumed to be the same:

(26) Dorman, D. E.; Roberts, J. D. *Proc. Natl. Acad. Sci. U.S.A.* **1970**, *65*, 19–26.

(27) Mueller, L. *J. Am. Chem. Soc.* **1979**, *101*, 4481–4484.

(20) Peng, J. W.; Wagner, G. *Methods Enzymol.* **1994**, *239*, 563–596.  
(21) Jardetzky, O.; Roberts, G. C. K. *NMR in Molecular Biology*; Academic Press, Inc.: Orlando, 1981; pp 115–142.

(22) Legault, P. Ph. D. Thesis, University of Colorado at Boulder, 1995.  
(23) Nikonowicz, E. P.; Sirt, A.; Legault, P.; Jucker, F. M.; Baer, L. M.; Pardi, A. *Nucleic Acids Res.* **1992**, *20*, 4507–4513.

(24) Cohn, W. E. *J. Am. Chem. Soc.* **1950**, *72*, 1471–1478.

(25) Milligan, J. F.; Groebe, D. R.; Witherell, G. W.; Uhlenbeck, O. C. *Nucleic Acids Res.* **1987**, *15*, 8783–9798.

(28) Marion, J.; Ikura, M.; Tschudin, R.; Bax, A. *J. Magn. Reson.* **1989**, *85*, 393–399.

(29) Simorre, J. P.; Zimmermann, G. R.; Pardi, A.; Farmer, B. T., II; Mueller, L. *J. Biomol. NMR* **1995**, *6*, 427–432.

(30) Wyman, J.; Gill, S. J. *Binding and Linkage. Functional Chemistry of Biological Macromolecules*; University Science Books: Mill Valley, CA, 1990; pp 33–122.

(31) Gutowsky, H. S.; Holm, C. H. *J. Chem. Phys.* **1956**, *25*, 1228–1234.

**Table 1.** Maximum Changes in  $^{13}\text{C}$  Chemical Shifts ( $\delta$  (pH<sub>f</sub>) -  $\delta$  (pH<sub>i</sub>) in ppm) with pH for the  $^{13}\text{C}/^{15}\text{N}$ -Labeled 5' NMPs

carbon type	$\delta$ (pH <sub>f</sub> ) - $\delta$ (pH <sub>i</sub> )			
	5' AMP pH <sub>i</sub> = 2.1 pH <sub>f</sub> = 7.3	5' CMP pH <sub>i</sub> = 2.6 pH <sub>f</sub> = 7.5	5' GMP pH <sub>i</sub> = 7.1 pH <sub>f</sub> = 12.3	5' UMP pH <sub>i</sub> = 7.1 pH <sub>f</sub> = 12.3
C8	-2.2		-2.1	
C6	5.6	-2.1	9.2	-1.5
C5	0.0	1.5	1.3	0.5
C4	0.7	7.1	0.0	10.8
C2	8.2	9.4	7.3	7.9
C5'	-0.8	-0.7	0.1	0.2
C4'	0.5	0.2	-0.2	-0.6
C3'	0.4	0.6	0.2	0.2
C2'	-0.2	0.0	0.1	-0.1
C1'	-1.2	-0.6	-0.5	0.4

$$\nu(f) \propto \frac{[P(1 + \tau_{ce}(p_A\omega_B + p_B\omega_A)) + QR]}{P^2 + R^2} \quad (1)$$

where  $\tau_{ce} = \tau_A\tau_B/(\tau_A + \tau_B)$ ,  $1 = p_A + p_B$ ,  $\omega_N = \pi^*lw_N$ ,  $lw_N$  = line width at half-height of state N,  $P = \tau_{ce}[\omega_A\omega_B - (\pi(f_A + f_B) - 2\pi f)^2 + \pi^2(f_A - f_B)^2] + p_A\omega_A + p_B\omega_B$ ,  $Q = \tau_{ce}[\pi(f_A + f_B) - 2\pi f - \pi(p_A - p_B)(f_A - f_B)]$ ,  $R = \pi(f_A - f_B)(p_A - p_B) - \tau_{ce}\pi(f_A - f_B)(\omega_A - \omega_B) + [\pi(f_A + f_B) - 2\pi f][1 + \tau_{ce}(\omega_A + \omega_B)]$  where  $\tau_{ce}$  is the lifetime for exchange,  $\tau_N$ ,  $f_N$ , and  $p_N$  are the lifetime, the frequency (Hz), and the fractional population of the state N (either state A or B), respectively, and  $\nu(f)$  represents the signal intensity at a frequency  $f$  (Hz). An awk (AT&T Bell Laboratories) script that calculates the lineshape of a two-state system was used to extract the chemical shift and line width at half-height of the signal for a given lifetime of chemical exchange. The rate of exchange and its error were calculated by fitting the experimental chemical shift and line width at half-height with the calculated ones.  $p_A$  (population of protonated A25) and  $p_B$  (population of unprotonated A25) were derived from the chemical shift ( $\delta$ ) of the A25 C2 resonance using the conversions  $p_A = \Delta/\Delta_T$  and  $p_A + p_B = 1$ , where  $\Delta = 155.32 \text{ ppm} - \delta_{A25 \text{ C2}}$  (ppm) and  $\Delta_T = 7.78 \text{ ppm}$  (978 Hz) (Table 1).<sup>5</sup>  $lw_B$  is the line width at half-height of the unprotonated state and was measured to be  $27 \pm 3 \text{ Hz}$  at pH 8.45, and  $lw_A$  is the line width at half-height of the protonated state measured and was  $37 \pm 15 \text{ Hz}$  at pH 4.20. These line widths were not affected by  $^{13}\text{C}$ - $^{15}\text{N}$  J coupling constants which were less than 10 Hz at all pH values in 5' AMP (data not shown). The errors on the lifetime of exchange,  $\tau_{ce}$ , were estimated using errors of  $\pm 0.2 \text{ ppm}$  on the measured  $^{13}\text{C}$  chemical shift which was used to calculate  $p_A$  and  $p_B$ , and errors for the measured line widths at a given pH and at the extreme pH values (Table 3).

## Results

**pH Dependence of  $^{13}\text{C}$  Chemical Shifts and One-Bond  $^1\text{H}$ - $^{13}\text{C}$  Coupling Constants in 5' NMPs.** To search for  $^{13}\text{C}$  NMR probes that can be used to detect unusual  $pK_a$ 's in nucleic acids, the pH dependence of all  $^{13}\text{C}$  chemical shifts were determined in  $^{13}\text{C}/^{15}\text{N}$ -labeled 5' AMP, 5' GMP, 5' CMP, and 5' UMP by 1D  $^1\text{H}$ -decoupled  $^{13}\text{C}$  NMR spectra. The results for the aromatic C2, C4, C6, and C8 resonances are presented in Figure 1. For all four nucleotides, there is at least one base carbon chemical shift that changes by at least 8 ppm over the pH range studied, whereas the ribose carbon chemical shifts change by  $\leq 1.2 \text{ ppm}$  (Table 1). These results are consistent with previously published two data-point pH studies for 5' CMP, 5' ATP, adenine, and cytosine.<sup>26,32</sup> The C2 and C6 of adenine and guanine and the C2 and C4 of cytosine and uridine are the most sensitive  $^{13}\text{C}$  NMR probes for  $pK_a$  determinations. The  $pK_a$ 's of all four 5' NMPs were estimated from Hill plot analysis based on the change of the chemical shifts of these carbons (not shown) and agree with values published previously for the

**Table 2.** Maximum Change in One-Bond  $^1\text{H}$ - $^{13}\text{C}$  Coupling Constants with pH for the  $^{13}\text{C}/^{15}\text{N}$ -Labeled 5' NMPs<sup>a</sup>

one-bond coupling	max. change in one-bond $^1\text{H}$ - $^{13}\text{C}$ coupling constant (Hz) error is $\pm 0.4 \text{ Hz}$
A H2-C2	-13.4
A H8-C8	-2.4
A H1'-C1'	-2.0
G H8-C8	-2.3
G H1'-C1'	-1.5
C H6-C6	-3.8
C H5-C5	-6.9
C H1'-C1'	-2.9
U H6-C6	-3.7
U H5-C5	-6.7
U H1'-C1'	-2.8

<sup>a</sup> Maximum differences in one-bond proton-carbon coupling constants were obtained from 1D  $^1\text{H}$  NMR spectra obtained at extreme pH values. For 5' AMP, the difference is calculated as  $J_{pH7.3} - J_{pH2.1}$ , for 5' GMP and 5' UMP as  $J_{pH12.3} - J_{pH7.1}$ , and for 5' CMP as  $J_{pH7.5} - J_{pH2.6}$ .

titration of the imino nitrogens.<sup>15</sup> In all cases the slope obtained for the Hill plot was  $1.0 \pm 0.1$  as expected for a single protonation event. The protonation of the 5' monophosphate which has a  $pK_a$  around 6.8<sup>15</sup> does not have any detectable effect on the C2, C4, C6, and C8 chemical shifts (Figure 1). These results demonstrate that the C2 and C6 resonances of purines and the C2 and C4 resonances of pyrimidines can be used to monitor accurately the protonation of the imino nitrogen for the four common nucleotides.

The effects of base protonation on  $^1J_{\text{CH}}$  coupling constants were measured for the aromatic protons of the  $^{13}\text{C}/^{15}\text{N}$ -labeled 5' NMPs. Except for the H2-C2 coupling constant of 5' AMP and the H5-C5 coupling constants of 5' CMP and 5' UMP no substantial pH-dependent changes in  $^1J_{\text{CH}}$  coupling constants were observed (Table 2). For A H2-C2, U H5-C5, and C H5-C5, the change in proton-carbon coupling constant with pH directly reflects the imino protonation (not shown).

**Measurement of  $pK_a$ 's in the Leadzyme.** 2D ( $^{13}\text{C}$ ,  $^1\text{H}$ ) HMQC spectra were collected at multiple pH values and used to monitor the aromatic C2-H2 region of the leadzyme as a function of pH, and these spectra are similar to those previously published (see Figure 2 in ref 5). The pH titration plots for all adenine C2s in the leadzyme are shown in Figure 2a. A detailed analysis of the pH titration study of A25 C2 was published previously.<sup>5</sup> It was not possible to obtain a complete pH titration curve for the other adenines in the range of pH studied, because we did not want to subject the RNA to very extreme pH's (Figure 2a). However, we can estimate their  $pK_a$ 's from the maximum change in C2 chemical shift between pH 8.3 and 4.4 assuming that no pH-dependent effect other than imino nitrogen protonation contributes to the pH-induced change in  $^{13}\text{C}$  chemical shifts. A summary of all adenine  $pK_a$ 's for the leadzyme is given in Figure 2b.

To test for protonated cytidines in the leadzyme a 2D (HN)C-(CC)H spectrum was collected on the leadzyme at pH 5.5 where the C4 resonances are frequency labeled in the  $t_1$  evolution period. This 2D spectrum is shown in Figure 3.

**Calculating the Lifetime of Exchange for Protonation-Deprotonation of A25.** Chemical exchange on the chemical shift timescale is reflected in the lineshape of the detected signal where the exchanging nuclei experience two or more electronic environments.<sup>21</sup> In the leadzyme, the large line width for the C2 of A25 at various pH's indicates that this resonance is in intermediate exchange (as illustrated in Figure 2 in ref 5). Both

(32) Sierzputowska-Graczyk, H.; Gopal, H. D.; Agris, P. F. *Nucleic Acids Res.* **1986**, *14*, 7783-7801.

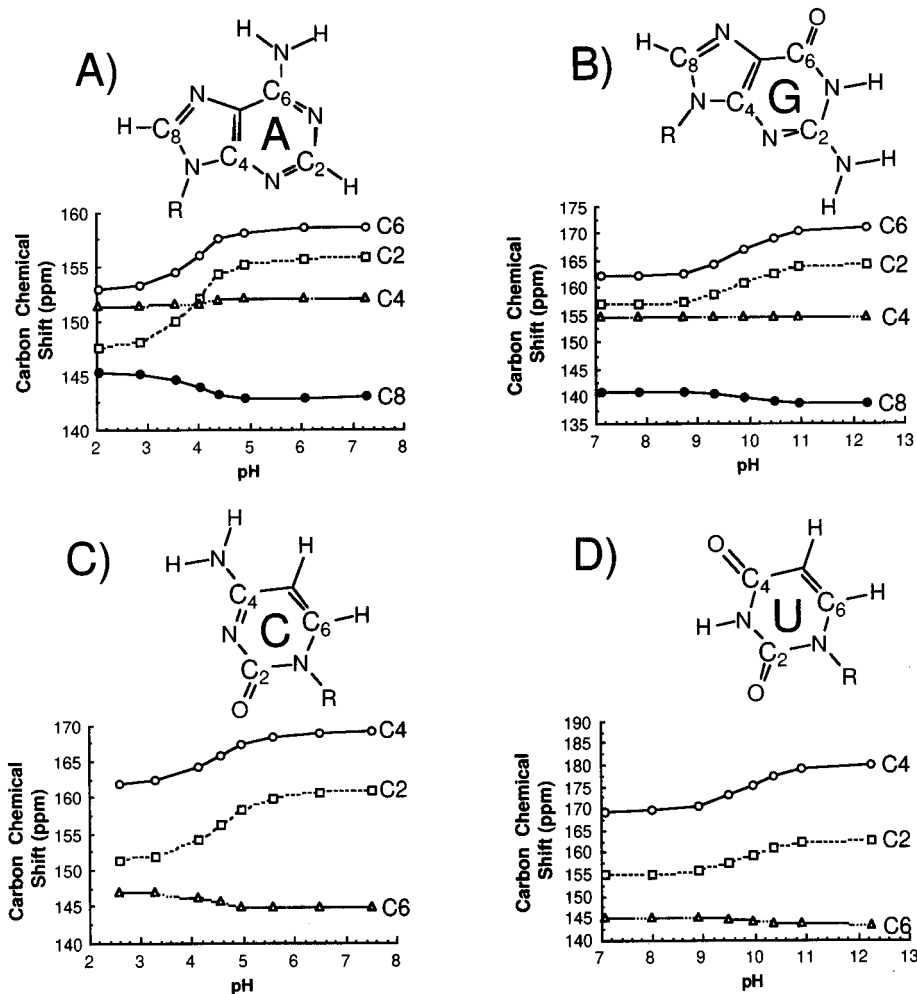


**Figure 1.** pH titration of  $^{13}\text{C}/^{15}\text{N}$ -labeled NMPs monitored by  $^{13}\text{C}$  NMR spectroscopy: (A) 5' AMP, (B) 5' GMP, (C) 5' CMP, and (D) 5' UMP. The individual bases are shown above the titration plots.

the line width and chemical shift of A25 depend on the populations, line widths, and rate of exchange between the protonated and the unprotonated states.<sup>31</sup> 2D ( $^{13}\text{C}$ ,  $^1\text{H}$ ) HSQC spectra of the leadzyme were collected at six pH values, and line widths at half-height were measured from the  $^{13}\text{C}$  vectors (Table 3). For A25 the C2 lineshapes are broader at intermediate pH than at the extreme pH's. In the range of pH's studied, the  $^{13}\text{C}$  line width of A12 C2 in the leadzyme does not vary which indicates that the overall relaxation properties of the leadzyme do not change enough to affect the carbon line widths. Therefore the observed variations in the A25 C2 line widths are simply caused by the protonation equilibrium.

The slope of 1 obtained from the Hill plot of A25 protonation<sup>5</sup> validates a two-state model between the unprotonated and protonated forms of A25 and justifies the use of eq 1 for the determination of the lifetime of chemical exchange associated with A25 protonation. This equation was therefore used to estimate the lifetime of chemical exchange from the line width of A25 C2 at the four pH values of 5.50, 5.85, 6.55, and 7.63 (Table 3). The line widths of A25 C2 at pH 4.20 and pH 8.45 represent the line widths of the fully protonated and fully unprotonated states, respectively. The fractional populations of the protonated ( $p_A = (155.32 \text{ ppm} - \delta_{\text{pHx}})/7.78$ ) and unprotonated ( $p_B = 1 - p_A$ ) forms were determined from the chemical shift of A25 C2 at a given pH ( $\delta_{\text{pHx}}$ ). As seen in Table 3, the lifetime of exchange is independent of pH within error, with  $\tau_{\text{ce}} = 31 \pm 8 \mu\text{s}$  which corresponds to a rate of exchange of  $k_{\text{ce}} = 1/\tau_{\text{ce}} = 3.2 \pm 1.1 \times 10^4 \text{ s}^{-1}$ .

## Discussion

**Detection of Unusual  $\text{pK}_a$ 's in Nucleic Acids.** Although base protonation affects the  $^1\text{H}$ ,  $^{15}\text{N}$ , and  $^{13}\text{C}$  chemical shifts in mononucleotides,<sup>5,33,34</sup> the effects on the  $^{13}\text{C}$  and  $^{15}\text{N}$  shifts are much larger than the  $^1\text{H}$  shifts and are therefore less influenced by environmental factors other than base protonation. Thus,  $^{15}\text{N}$  and  $^{13}\text{C}$  chemical shifts provide superior probes for detecting shifted base  $\text{pK}_a$ 's in nucleic acids. The pH dependences of  $^{15}\text{N}$  chemical shifts in 3' NMPs have shown that the N1 chemical shifts of GMP and AMP and the N3 chemical shifts of CMP and UMP change dramatically (40–70 ppm) upon protonation of the imino nitrogen and that these are the only nitrogen chemical shifts that are significantly affected by pH.<sup>34</sup> Essentially complete NMR assignment of the proton, protonated carbon, and protonated nitrogen resonances have been made for the leadzyme at pH 5.5<sup>22</sup> which then makes it possible to use the NMR chemical shifts as probes of unusual base  $\text{pK}_a$ 's in this system. All the A N1s, U N3s, and G N1s were assigned except for A18 N1, A25 N1, G7 N1, G9 N1, and G24 N1 where chemical exchange broadening or rapid  $^{15}\text{N}$  relaxation led to inefficient transfer of magnetization.<sup>22</sup> All the assigned A, U, and G imino nitrogens in the leadzyme lie within a narrow range of 5 ppm for each base type at pH 5.5 (data not shown).

(33) Sowers, L. C.; Fazakerley, G. V.; Kim, H.; Dalton, L.; Goodman, M. F. *Biochemistry* **1986**, *25*, 3983–3988.

(34) Büchner, P.; Maurer, W.; Rüterjans, H. *J. Magn. Reson.* **1978**, *29*, 45–63.

**Table 3.** Data Used for Calculation of Exchange Times in the Leadzyme at 25 °C

pH	A12 C2 chemical shift <sup>b</sup> (ppm)	A12 C2 line width at half-height <sup>b</sup> (Hz)	A25 C2 chemical shift <sup>b</sup> (ppm)	A25 C2 line width at half-height <sup>b</sup> (Hz)	A25 fractional populations <sup>a</sup> $p_A/p_B$	exchange time for A25 ( $\mu$ s)
4.20	152.5	25 $\pm$ 3	147.7	37 $\pm$ 15	0.995/0.005	
5.50 <sup>c</sup>	152.5	23 $\pm$ 1	148.3	59 $\pm$ 1	0.898/0.102	28 $\pm$ 4
5.85	152.5	25 $\pm$ 1	149.0	87 $\pm$ 18	0.812/0.188	29 $\pm$ 13
6.55	152.5	26 $\pm$ 1	151.7	144 $\pm$ 14	0.465/0.535	37 $\pm$ 5
7.63	152.5	24 $\pm$ 1	154.8	46 $\pm$ 5	0.067/0.933	28 $\pm$ 8
8.45	152.5	26 $\pm$ 2	155.2	27 $\pm$ 3	0.011/0.989	

<sup>a</sup> The fractional populations were calculated from A25 C2 chemical shifts (see Material and Methods):  $p_A$  = population of protonated A25,  $p_B$  = 1 -  $p_A$ . <sup>b</sup> The chemical shifts and line width were measured from 1D <sup>13</sup>C vector of (<sup>13</sup>C, <sup>1</sup>H) HSQC spectra (see text). Errors on line widths at half-height were estimated from fitting to a Lorentzian line and varied depending upon the signal-to-noise of the peak. <sup>c</sup> The data at pH 5.50 were measured in a 2D (<sup>13</sup>C, <sup>1</sup>H) HSQC spectrum taken on the 1.2 mM <sup>13</sup>C/<sup>15</sup>N-labeled leadzyme. This spectrum had higher signal to noise than the data at the other pH values which yielded higher precision for measurement of the line widths of the 1D <sup>13</sup>C cross sections.

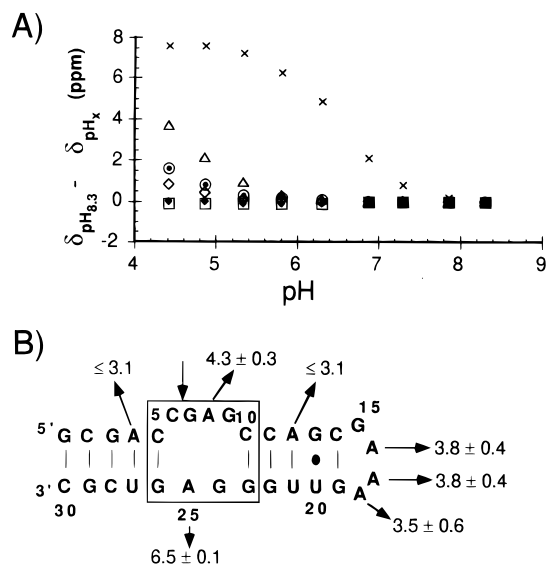


**Figure 2.** (A) pH titration curve of A25 (cross), A8 (open triangles), A16 (open circle), A17 (filled circle), A18 (open diamond), A4 (filled diamond), and A12 (open square) C2 chemical shifts. The y axis is the difference in <sup>13</sup>C chemical shift between the unprotonated form and the chemical shift at the given pH. (B) Summary of the estimated  $pK_a$ 's in the leadzyme (see Materials and Methods). The sequence and secondary structure of the leadzyme are shown where the boxed region indicates the residues that are required for cleavage, and the arrow indicates the site of cleavage.<sup>18,19</sup>

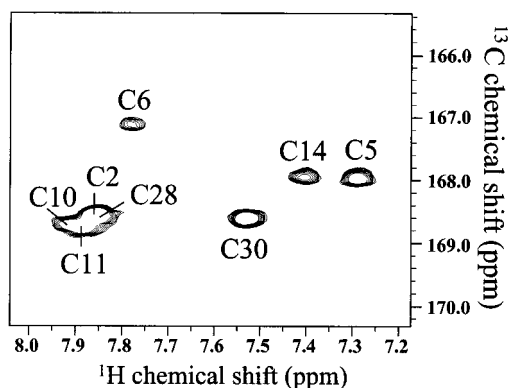


**Figure 3.** A contour plot of the C4 to H6 region of the cytidine-specific 2D (<sup>13</sup>C, <sup>1</sup>H) (HN)C(CC)H spectrum of the 1.2 mM uniformly <sup>13</sup>C/<sup>15</sup>N-labeled leadzyme at pH 5.5. The spectrum was collected as previously described except that the carbon evolution period was set for frequency labeling of the C4 resonances.<sup>29</sup>

Therefore, for these observed imino nitrogens there is no indication of perturbed  $pK_a$  values at this pH in the leadzyme.<sup>22</sup>

As seen in Figure 1 the carbons directly bonded to the nitrogen that becomes protonated (the C2 and C6 of purines

and the C2 and C4 of pyrimidines) are the most sensitive <sup>13</sup>C NMR probes for monitoring the imino protonation in RNA since the chemical shifts of these carbons undergo the largest changes upon protonation. The chemical shift changes for these carbons between the unprotonated and protonated states range from +5.6 to +10.8 ppm (Figure 1 and Table 1). The sign and magnitude of these changes agree with theoretical and experimental studies of azines (six-membered nitrogen heterocycles) where the directly bound carbons undergo a +8 ppm upfield shift upon nitrogen protonation.<sup>35</sup> The adenine C2 is directly bound to a proton and is easily detected by a 2D (<sup>13</sup>C, <sup>1</sup>H) HMQC or HSQC experiment. Thus for adenine the C2 represents the best probe of base protonation. For cytosine and uridine, C2 and C4 are not protonated carbons, and, therefore, these carbons were previously not routinely assigned, even in <sup>13</sup>C labeled molecules. However we have recently developed a series of base-specific triple resonance experiments for assignment of the exchangeable and nonexchangeable base protons in <sup>13</sup>C/<sup>15</sup>N nucleic acids.<sup>29,36,37</sup> A 2D H(NCCC)H experiment was previously used to provide H<sub>2</sub>N to H6 connectivities for the cytidines in the leadzyme.<sup>29</sup> A similar experiment can be used to assign the C4 resonances in cytidines and Figure 3 shows the 2D (<sup>13</sup>C, <sup>1</sup>H) (HN)C(CC)H experiment that was used to assign the cytidine C4 resonances in the leadzyme at pH 5.5. Comparison of this spectrum with the pH dependence of C4 in the 5' CMP (Figure 1) shows that all the leadzyme cytidine C4 resonances have chemical shifts consistent with the unprotonated species. The C4 resonance of residue C6 shows the largest deviation from the chemical shift of the mononucleotide, but this residue forms a base pair with the protonated A25 as discussed below. Formation of the A25H<sup>+</sup>-C6 base pair is likely leading to the slightly perturbed chemical shift for the C4 resonance of residue C6. Thus the chemical shifts of the C4 resonances (Figure 3) indicate that there are no cytidine residues with unusually high  $pK_a$ 's in the leadzyme.

#### In Situ Measurement of Adenine $pK_a$ 's in the Leadzyme.

Figure 2 shows the  $pK_a$ 's for the adenine bases in the leadzyme. These  $pK_a$ 's fall in three general classes when compared with the  $pK_a$  of 5' AMP. 1)  $pK_a$ 's that are similar to the  $pK_a$  of 5' AMP are found for the adenines in the GAAA loop and for A8 in the internal loop region. NMR solution and X-ray crystal structures of GAAA loop have been determined and show that the imino nitrogens of the three adenines in the loops are solvent accessible.<sup>38-41</sup> Thus the  $pK_a$ 's of these adenines are expected to be similar to the  $pK_a$  of 5' AMP. For A8 in the internal

(35) Pugmire, R. J.; Grant, D. M. *J. Am. Chem. Soc.* **1968**, *90*, 697-706.

(36) Simorre, J. P.; Zimmermann, G. R.; Mueller, L.; Pardi, A. *J. Am. Chem. Soc.* **1996**, *118*, 5316-5317.

(37) Simorre, J. P.; Zimmermann, G. R.; Mueller, L.; Pardi, A. *J. Biomol. NMR* **1996**, *7*, 153-156.

(38) Heus, H. A.; Pardi, A. *Science* **1991**, *253*, 191-194.

loop, having a  $pK_a$  similar to AMP indicates that this imino proton is also accessible to solvent. Our current three-dimensional structure of the leadzyme is consistent with the imino nitrogen of A8 being solvent accessible.<sup>42</sup> (2) A4 and A12 have  $pK_a$ 's that are lower than the  $pK_a$  of 5' AMP. These residues are involved in standard Watson–Crick base pairs. The lower  $pK_a$ 's mean that formation of a stable base pair makes it more difficult to protonate the adenine. Thus the helix-coil transition equilibrium affects the protonation equilibrium. This result is similar to what is observed for hydrogen exchange experiments where the G and U imino proton hydrogen exchange rates are slower in base pairs relative to solvent-exposed bases.<sup>43,44</sup> (3) The  $pK_a$  of 6.5 for A25 is 2.5 pH units higher than that of 5' AMP and is close to physiological pH.<sup>5</sup>

Many potential structural roles could be attributed to A25. A protonated adenine could stabilize the formation of base pairing interactions by direct hydrogen bonding of its imino proton. A large number of interaction schemes are possible but to our knowledge the A imino hydrogen has been found to form hydrogen bonds only in specific types of  $AH^+–C$ <sup>3,4,6</sup> and  $AH^+–G$ <sup>8,45,46</sup> base pairs and in the  $AH^+–G–C^2$  base triple (Figure 4a). A  $pK_a$  of 6.6 has been reported for an  $AH^+–C$  wobble base pair in a DNA oligomer,<sup>4</sup> and a  $pK_a$  of 6.2 was measured for a  $AH^+–C$  wobble base in an internal loop in a domain of the hairpin ribozyme.<sup>14</sup> We are presently refining the 3D structure of the leadzyme,<sup>42</sup> and these structural data indicate that the same type of  $AH^+–C$  wobble base pair<sup>3,4,6</sup> is forming between C6 and A25 in the internal loop in the leadzyme (see Figure 4A). Another possibility that could lead to an increased  $pK_a$  for A25 is if the imino proton is involved in the formation of a “salt-bridge” or stabilizing interaction with a negatively charged phosphate. Such interactions have been proposed for  $AH^+–A$  and  $AH^+–G$  base pairing in DNA oligomers<sup>47</sup> and in poly( $AH^+$ )-poly(A)<sup>15,48</sup> (Figure 4b). In these cases, the protonated adenine most likely helps to neutralize a local negative potential.<sup>48</sup> The amino protons in adenine become more acidic upon N1 protonation<sup>49</sup> which could then form stronger hydrogen bonds. More stable hydrogen-bonding interactions with the amino protons could also result from the restricted rotation of the carbon-amino nitrogen bond which gains additional double-bond character upon N1 protonation.<sup>50</sup> It has also been proposed that the change in the dipole moment of the protonated adenine, compared to its neutral form, favors particular stacking interactions.<sup>47</sup>

Although the structural data indicate formation of a  $A25H^+–C6$  wobble base pair in the leadzyme,<sup>42</sup> the potential roles for a protonated adenine in RNA are not strictly structural. The presence of a base with a  $pK_a$  close to physiological pH and in

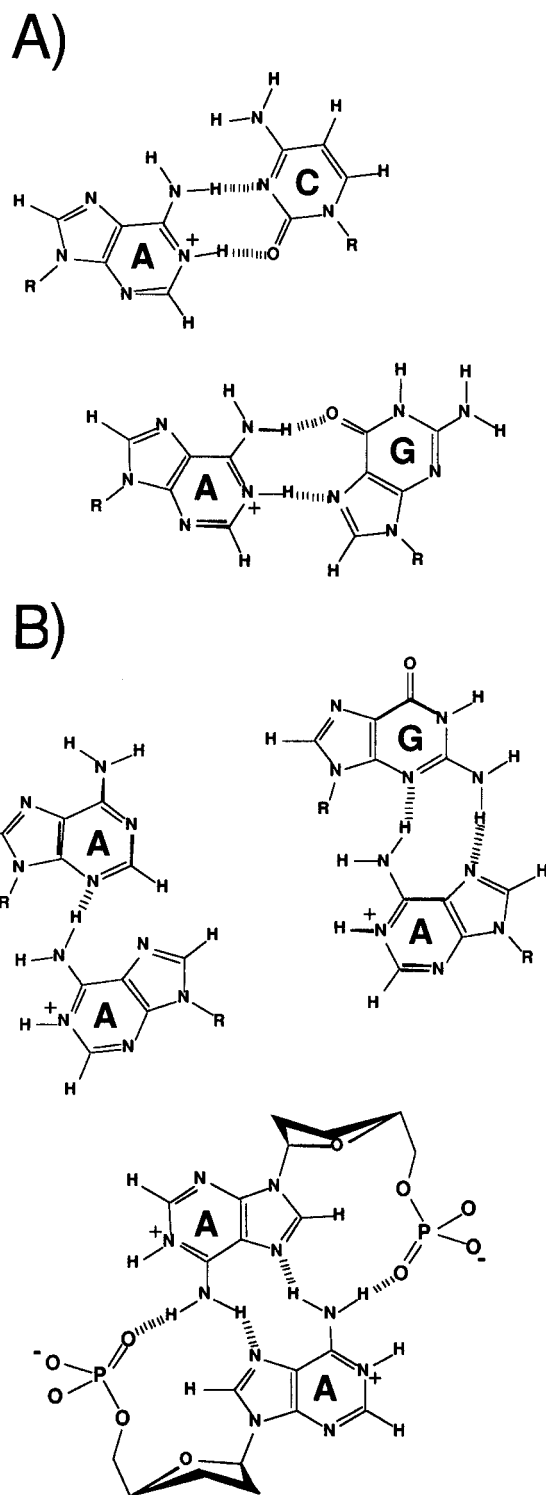


**Figure 4.** Structures of previously proposed nucleic acid base pair interactions involving protonated adenines. (A) The imino proton of the protonated adenine can directly participate in hydrogen-bonding interactions in  $AH^+–C$ <sup>3,4,6</sup> and  $AH^+–G$  base pairs.<sup>8,45,46</sup> (B) The protonated adenine can also form stable interactions without its imino proton being directly involved in an interbase hydrogen bond, as in the  $AH^+–A$  base pairs<sup>15,47,48,61</sup> and  $AH^+–G$  base pairs.<sup>47</sup>

proximity to the cleavage site (Figure 2b) could play various roles in catalysis. For example, (1) the positively charged A25 could stabilize the formation of a negatively charged transition state; (2) the imino proton of A25 could be involved in general acid catalysis,<sup>51</sup> but this role could also be ascribed to the amino protons since the  $pK_a$  of the adenine amino proton decreases from 20 to around 8 upon N1 protonation;<sup>52,53</sup> (3) the protonated

(39) Pley, H. W.; Flaherty, K. M.; McKay, D. B. *Nature* **1994**, *372*, 111–113.

(40) Jucker, F. M.; Heus, H. A.; Yip, P. F.; Moors, E. H. M.; Pardi, A. *J. Mol. Biol.* **1996**, *264*, 968–980.

(41) Jucker, F. M.; Pardi, A. *RNA* **1995**, *1*, 219–222.

(42) Hoogstraten, C. G.; Legault, P.; Pardi, A. Unpublished results.

(43) Nonin, S.; Leroy, J. L.; Guéron, M. *Biochemistry* **1995**, *34*, 10652–10659.

(44) Englander, S. W.; Kallenbach, N. R. *Q. Rev. Biophys.* **1984**, *16*, 521–655.

(45) Carbonnaux, C.; van der Marel, G. A.; van Boom, J. H.; Guschlbauer, W.; Fazakerley, G. V. *Biochemistry* **1991**, *30*, 5449–5458.

(46) Leonard, G. A.; Booth, E. D.; Brown, T. *Nucleic Acids Res.* **1990**, *18*, 5617–5623.

(47) Maskos, K.; Gunn, B. M.; LeBlanc, D. A.; Morden, K. M. *Biochemistry* **1993**, *32*, 3583–3595.

(48) Rich, A.; Davies, D. R.; Crick, F. H. C.; Watson, J. D. *J. Mol. Biol.* **1961**, *3*, 71–86.

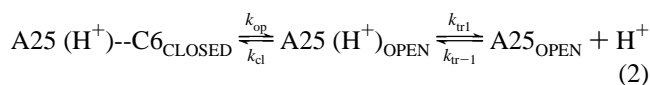
(49) Guéron, M.; Leroy, J. L. *Meth. Enzymol.* **1995**, *261*, 383–413.

(50) Shoup, R. R.; Miles, H. T.; Becker, E. D. *J. Chem. Phys.* **1972**, *76*, 64–70.

A25 could aid in the proper positioning of the  $\text{Pb}^{2+}$  for cleavage by creating unfavorable electrostatic interactions with the positively charged metal. Although the  $\text{p}K_a$  of 6.5 for A25 was determined in the absence of divalent metals,<sup>5</sup> addition of 1 mM  $\text{Pb}^{2+}$  to the NMR sample does not significantly change the NMR spectra except for a shift of the A25 C2 resonance by 0.7 ppm at pH 5.5. Using the equation for the pH dependence of A25 C2 determined in the absence of  $\text{Pb}^{2+}$ , we find a  $\text{p}K_a$  of 6.3 for A25 under conditions with 1 mM  $\text{Pb}^{2+}$ . These results indicate that  $\text{Pb}^{2+}$  does not affect the structure and only slightly shifts the  $\text{p}K_a$  of A25.

There are also other indications that the protonated A25 is involved in a structural and not a catalytic role in the leadzyme. The log linear pH dependence of the cleavage rate between pH 5.5 and 7.0<sup>19</sup> does not support the requirement of A25 protonation to reach the transition state. In addition, A25 can be replaced by C or U, and the extent of cleavage is reduced by less than a factor of 2.<sup>19</sup> In most protein enzymes, replacement of an amino acid that plays a critical role in the chemistry of reaction decreases the reaction rate.<sup>1</sup>

**Dynamics at the Active Site of the Leadzyme.** Analysis of the line width for the C2 resonance of A25 demonstrates that this base is undergoing exchange between its protonated and unprotonated forms with a lifetime of  $\sim 30 \mu\text{s}$ . To help understand this exchange process we considered the reaction scheme used in imino proton exchange studies<sup>44</sup> to describe hydrogen exchange of the imino proton of A25 assuming that A25 is base-paired with C6:



where  $k_{\text{op}}$  and  $k_{\text{cl}}$  are the base pair opening and closing rate constants respectively, and  $k_{\text{tr1}}$  and  $k_{\text{tr}-1}$  represent the forward and reverse rates of proton transfer for the open state of the base pair. In this scheme it is assumed that no hydrogen exchange takes place from the base-paired (closed) state. There are several pieces of evidence that support the hypothesis that  $k_{\text{op}}$  is the rate limiting step in eq 2, under our conditions. The most likely mechanism for protonation and deprotonation of A25 would be acid or base catalyzed exchange and the rate ( $k_{\text{tr1}}$  or  $k_{\text{tr}-1}$ ) would be proportional to the concentration of the catalyst.<sup>44</sup> Under these conditions the imino proton exchange rates would be pH dependent because the concentrations of any potential exchange catalyst (proton, hydroxide or phosphate buffer) would change as a function of pH. However as seen in Table 3 the lifetime for the exchange process of A25 is not pH dependent. In addition the measured exchange broadening of the C2 resonance of A25 is the same in 10 mM sodium phosphate buffer, pH 5.5, as it is in 25 mM succinate-*d*<sub>4</sub> buffer, pH 5.5 (data not shown). Thus the lack of buffer and pH dependence of the observed exchange rate for A25 is consistent with  $k_{\text{op}}$  being the rate limiting step in the exchange.

If opening of the proposed  $\text{A25H}^+\text{-C6}$  base pair is the rate limiting step for the hydrogen exchange process in eq 2 then  $k_{\text{op}} = k_{\text{ce}} \approx 3 \times 10^4 \text{ s}^{-1}$ . This rate is faster than rates of individual nonterminal Watson-Crick G-C or A-U base-pair opening in DNA duplexes which are on the order of  $10^2 \text{ s}^{-1}$  at 25 °C.<sup>54</sup> The imino proton resonance for a  $\text{AH}^+\text{-C}$  base would be expected to have a chemical shift of 15–16 ppm,<sup>55</sup> and no

such resonance is observed in the NMR spectrum of the leadzyme, even at a pH as low as 5.0 (not shown). This means the hydrogen exchange of the A25 imino proton is fast on the <sup>1</sup>H NMR chemical shift timescale which is also consistent with  $k_{\text{tr1}} > 3 \times 10^4 \text{ s}^{-1}$ .

As seen in Table 3, under many of the NMR conditions a substantial fraction of the A25 base is protonated and forms a  $\text{A25H}^+\text{-C6}$  base pair. In fact, if the elevated  $\text{p}K_a$  of 6.5 is completely caused by the stabilization of the protonated form in a base paired and the  $\text{p}K_a$  of A25 in the open state is equal to the  $\text{p}K_a$  of AMP, it can be shown that  $K_{\text{a(A25)}} = K_{\text{a(AMP)}}(k_{\text{op}}/k_{\text{cl}})$  and that the dissociation equilibrium constant  $K_{\text{op}} = k_{\text{op}}/k_{\text{cl}} = 3 \times 10^{-3}$ . If  $k_{\text{op}}$  is the rate limiting step for the hydrogen exchange then  $k_{\text{op}} = 3 \times 10^4 \text{ s}^{-1}$  which yields a value of  $k_{\text{cl}}$  of  $10^7 \text{ s}^{-1}$ . This value of  $k_{\text{cl}}$  is in agreement with previous estimates of base pair closing rates.<sup>49</sup> A dissociation constant  $K_{\text{op}}$  of  $10^{-3}$  is indicative of a weak base pair since dissociation constants of  $10^{-5}$ – $10^{-6}$  have been measured from individual G-C and A-U base pairs within stable helices,<sup>49</sup> and much larger values ( $\sim 1$ – $10^{-2}$ ) have been measured for Watson-Crick base pairs at the termini of helices<sup>43</sup> which are subject to fraying. From this analysis, the fraction in the open state for the proposed  $\text{A25H}^+\text{-C6}$  base pair in the leadzyme is larger than the fraction in the open state for standard Watson-Crick base pairs and is more comparable to a terminal base pair in a double helix.

Cai and Tinoco have recently determined the structure of the loop A domain of the hairpin ribozyme and found that the internal loop in this molecule contains a  $\text{AH}^+\text{-C}$  wobble base pair with this adenine having a  $\text{p}K_a$  of 6.2.<sup>14</sup> Although the <sup>13</sup>C chemical shift differences for the adenine C2 in this loop A are very similar to those previously observed in the leadzyme,<sup>5</sup> the dynamics manifested by the adenine in the leadzyme and in the loop A of the hairpin ribozyme are very different. In the hairpin loop domain the <sup>13</sup>C and <sup>1</sup>H resonances are both in slow exchange on the NMR timescale, and separate cross peaks are observed at intermediate pH for the protonated and unprotonated states of the adenine involved in the  $\text{AH}^+\text{-C}$  base pair.<sup>14</sup> This allowed Cai and Tinoco to determine that the rate of exchange between the protonated and unprotonated forms of this adenine was  $< 15 \text{ s}^{-1}$ . In the leadzyme the protonated and unprotonated forms of A25 are in intermediate to fast exchange on the <sup>1</sup>H and <sup>13</sup>C NMR timescale and the exchange rate is  $3.2 \times 10^4 \text{ s}^{-1}$ . Thus the exchange process for the protonated adenine in the leadzyme has a rate at least 2000 faster times than that observed in the loop A of the hairpin ribozyme. In both the leadzyme and the loop A, the  $\text{AH}^+\text{-C}$  base pairs stack on one side with a C-G base pair. However in the loop A the  $\text{AH}^+\text{-C}$  also stacks with a sheared G-A base pair, whereas no other stable base pairs are formed for the internal loop in the leadzyme.<sup>42</sup> If  $\text{AH}^+\text{-C}$  base pairs are undergoing the same exchange process in these two systems, then the dynamics is much more rapid in the leadzyme than in the loop A.

## Conclusion

The <sup>13</sup>C NMR methods presented here provide an important probe of shifted  $\text{p}K_a$ 's in nucleic acids as demonstrated for the A25 at the active site of the leadzyme. The  $\text{p}K_a$ 's of adenines A4 and A12 which form stable Watson-Crick A-U base pairs were found to be lower (both  $\leq 3.1$ ) than the  $\text{p}K_a$  of 5' AMP ( $\text{p}K_a = 4.0$ ). The stable helical structure hindered the protonation of these adenines at lower pH, thereby affecting the apparent protonation equilibrium. A similar situation is pro-

(51) Jencks, W. P. *Catalysis in Chemistry and Enzymology*; Dover: New York, 1987; pp 163–239.

(52) Teitelbaum, H.; Englander, S. W. *J. Mol. Biol.* **1975**, *92*, 55–78.

(53) McConnell, B. *Biochemistry* **1974**, *13*, 4516–4523.

(54) Guéron, M.; Kochoyan, M.; Leroy, J.-L. *Nature* **1987**, *328*, 89–92.

(55) Wijmenga, S. S.; Mooren, M. M.; Hilbers, C. W. In *NMR of Macromolecules. A Practical Approach*; Roberts, G. C. K., Ed.; IRL Press: New York, 1993; pp 217–288.

posed here for A25 where the elevated  $pK_a$  of 6.5 is caused by the stabilization of the protonated form of the adenine within a  $AH^+-C$  wobble base pair. Thus the  $pK_a$  of the adenine base is *lowered* when the protonation disrupts formation of the base pair, and the  $pK_a$  of the adenine is *raised* when the protonation is required for formation of the base pair. In addition to the unusual  $pK_a$  for A25 its C2 resonance shows extensive pH-dependent linebroadening indicating that this base is involved in a chemical exchange process with a rate of  $3 \times 10^4 \text{ s}^{-1}$ . These results demonstrate how  $^{13}\text{C}$  NMR can be used to probe rapid dynamic processes in RNA. This rate is much faster than the observed rate of cleavage and hydrolysis in the leadzyme<sup>18</sup> and therefore does not represent a rate-limiting step in these reactions.

Because the  $pK_a$ 's of the four natural bases are far from physiological pH, they have been viewed as unlikely candidates for acid-base catalysis. Furthermore, because all characterized ribozymes require divalent metal ions for their catalytic activity, research has focused on their role as metalloenzymes.<sup>56–58</sup> The cleavage of a phosphodiester bond to give a 2'-3' cyclic phosphate and a 5' hydroxyl terminus is a reaction catalyzed by ribozymes (including the leadzyme and the hammerhead and hairpin ribozymes) and by many protein enzymes such as RNase A and RNase T1.<sup>59,60</sup> In these two proteins, two histidines at the active site act as acid and base catalysts in the reaction.<sup>59,60</sup> It is therefore plausible that RNAs could also have

evolved to catalyze RNA degradation via a general acid–base reaction mechanism. The  $^{13}\text{C}$  NMR probes described here make it possible to search for bases with  $pK_a$ 's near physiological pH which could be good candidates to function as a general acid or base in ribozyme catalysis.

**Acknowledgment.** We are indebted to Professor Maurice Guéron for valuable discussions and a critical reading of the manuscript. We also thank Lotus Moon-McDermott for preparation of the T7 RNA polymerase, Cecilia Fernandez for separation of the  $^{13}\text{C}/^{15}\text{N}$ -labeled NMPs, Dr. Jean-Pierre Simorre for collecting the 2D (HN)C(CC)H spectrum on the leadzyme, Dr. Ping Yip for providing the awk script to calculate the lifetime for exchange, and Dr. Jennifer Doudna for the leadzyme template. This work was supported by NIH Grant AI30726 and a NIH Research Career Development Award AI01051 to A.P.P.L. was supported by a NSERC 1967 Science and Engineering scholarship and a FCAR (Fonds pour la Formation de Chercheurs et l' Aide à la Recherche) scholarship. The 500 MHz NMR spectrometer was purchased with partial support from NIH Grant RR03283. We also thank the Colorado RNA Center for support of RNA research on the Boulder campus.

JA9640051

(59) Findlay, D.; Herries, D. G.; Mathias, A. P.; Rabin, B. R.; Ross, C. A. *Nature* **1961**, *190*, 781–784.

(60) Nishikawa, S.; Morioka, H.; Kim, H. J.; Fuchimura, K.; Tanara, T.; Uesugi, S.; Hakoshima, T.; Tomita, K.-i.; Ohtsuka, E.; Ikehara, M. *Biochemistry* **1987**, *26*, 8620–8624.

(61) Chou, S.-H.; Cheng, J.-W.; Fedoroff, O. Y.; Chuprina, V. P.; Reid, B. R. *J. Am. Chem. Soc.* **1992**, *114*, 3114–3115.

(56) Pyle, A. M. *Science* **1993**, *261*, 709–714.

(57) Yarus, M. *Science* **1988**, *240*, 1751–1758.

(58) Steitz, T. A.; Steitz, J. A. *Proc. Natl. Acad. Sci. U.S.A.* **1993**, *90*, 6498–6502.